Materiales de Construcción
Vol. 72, Issue 347, July-September 2022, e292
ISSN-L: 0465-2746
https://doi.org/10.3989/mc.2022.17721

Replacement of hydrated lime by lime mud-residue from the cellulose industry in multiple-use mortars production

H. Sangi-Gonçalves, D. Penteado-Dias✉, R. Castillo-Lara

LECIV - Civil Engineering Laboratory, UENF - State University of Northern Rio de Janeiro, (Rio de Janeiro, Brazil)
✉: dylmar@uenf.br

Received 2 December 2021
Accepted 24 March 2022
Available on line 5 September 2022

ABSTRACT: The pulp and paper industry increases every year in Brazil, providing an important country position in international market due to its production volume. However, because of this increasing, a large volume of wastes is generated. One of them is a lime mud, resulting from the Kraft chemical pulping production process. Thus, the aim of this study was to evaluate the replacement of hydrated lime by lime mud on laying and coating mortars production, in order to verify its feasibility for possible application in civil construction industry. The 100% hydrated lime replacement mortar reached a 28-day compressive strength of 5.84 MPa. Finally, the results obtained in the experimental program showed that the 100% hydrated lime replacement mortar by lime mud meets the normative requirements for multiple-use mortars.

KEY WORDS: Lime mud; Sustainable mortar; Waste recycling.

Citation/Citar como: Sangi-Gonçalves, H.; Penteado-Dias, D.; Castillo-Lara, R. (2022) Replacement of hydrated lime by lime mud-residue from the cellulose industry in multiple-use mortars production. Mater. Construcc. 72 [347], e292. https://doi.org/10.3989/mc.2022.17721.

RESUMEN: *Sustitución de cal hidratada por lodos de cal, residuo de la industria celulosa, en la producción de morteros de uso múltiple.* La industria de celulosa y papel crece año tras año en Brasil. Sin embargo, debido a este aumento, se genera un gran volumen de desechos. Uno de ellos es un lodo de cal, resultante del proceso de producción de pulpa química Kraft. Así, el objetivo de este estudio fue evaluar la sustitución de la cal hidratada por lodos de cal en la producción de morteros para colocación y revestimiento, con el fin de verificar su viabilidad para su posible aplicación en la industria de la construcción civil. El mortero con 100% de sustitución de cal hidratada por el residuo alcanzó 5,84 MPa de resistencia a la compresión a los 28 días. Finalmente, los resultados obtenidos en el programa experimental mostraron que el mortero con sustitución total de cal hidratada por lodo de cal cumple con los requisitos normativos para morteros de usos múltiples.

PALABRAS CLAVE: Lodo de cal; Mortero sostenible; Reciclaje de residuos.

1. INTRODUCTION

The fast increase in the industrial waste amount is one of the main reasons that has led countries to adopt stricter environmental and sustainable policies. In Brazil, for example, the enactment of the National Solid Waste Policy in 2010 was a milestone in this regard. This policy deals with waste management associated with logistics models, as well as being concerned with the destination of these wastes in reuse actions. In addition, it legislates on the waste final disposal in sanitary landfills in accordance to the operational procedure standardized by the Brazilian Association of Technical Norms (ABNT), which recommends the waste intermediate coverage in municipal solid waste landfills to control environmental aspects such as waste transport by wind, gas emission, odors and vectors presence. The National Solid Waste Policy establishes guidelines for increasing solid waste recycling, in order to reduce its volume in sanitary landfills, with a consequent increase in their useful life (1).

Solid waste management needs to be treated with great care, both from an environmental and industrial point of view, as well as from a public health one, so that these materials are disposed of in a safe and economical way or, preferably, are recycled. According to (2), the lack of integrated solid waste management policies and practices represents a threat for sustainable development in cities. Thus, one way to prevent an ecological unbalance is to use different types of waste as raw materials in the production of sustainable materials.

The use of industrial wastes for the development of new materials has been the subject of several researches in literature, as well as a theme of interest to the generating segments, since their management represents significant expenses, increasing occupation of spaces and responsibilities with the environmental legislation. In addition, the adaptation of several sectors to sustainable practices, such as waste reduction, reuse and recycling, improves the companies prestige, leads to attractive economic results and reduces the risk of environmental obligations.

In the field of civil construction, actions aimed at sustainability continue to face some resistance, both from companies in the sector as well as the consumer market. One of the great challenges of civil construction is to reduce the consumption of natural raw materials, as in the cement case, which production requires the exploration of high levels of natural resources worldwide. Another example is lime production, which requires the extraction of approximately 2 tons of limestone for each produced ton. Besides, it releases a large amount of carbon dioxide into the atmosphere (3, 4).

Lime is widely used in mortars in civil construction. In general, multiple-use mortars are composed of cement, lime and sand in amounts that vary according to their application, e.g. blocks laying, walls and ceilings covering, smoothing layers, among others. Thus, the search for alternatives that reduce lime consumption is important for sustainability in civil construction. In this perspective, the replacement of the hydrated lime, traditionally used in mortars, by lime mud – a waste from the pulp and paper industry - arises as a possible solution.

Lime mud is an inorganic solid waste generated by the pulp and paper industry during the reagents chemical recovery step in the Kraft process. This chemical process is the most common in the cellulosic pulp manufacture however, it generates a large volume of solid waste. This makes the process disadvantageous from an economic point of view, due to the costs of disposal in landfills, and inappropriate from a sustainable point of view, due to the environmental impact generated (5).

Lime mud is predominantly composed of CaO which is present in the form of $CaCO_3$. Therefore, it is worth noticing that the name of the residue studied here leads to an erroneous association with reactive lime ($Ca(OH)_2$), when, in fact, lime mud is predominantly formed by limestone itself, that is, an inert material.

Studies on pulp and paper industry waste incorporation in the development of building materials have been carried out, such as in fired bricks (6), geopolymers (7), concrete (8), composites (9) and Portland cement-based mortars (10).

The influence, on fresh and hardened states, of cement partial replacement by lime mud in mortars production was evaluated by (11). Cement dry mass was replaced by lime mud at levels of 0, 10, 20 and 30%. Mortars mechanical strength was measured at 7, 28 and 90 days and showed no significant differences among all evaluated compositions. Mortars capillarity was measured at a 90-minute period. The higher the mortars lime mud content, the lower the capillarity coefficient, a phenomenon attributed to the filler effect of lime mud, that is, filling capillary voids in cement matrix. (10) evaluated the influence of using lime mud as a partial substitute for cement in self-compacting mortars for floors. A reference mortar with a ratio of 1:3 (cement:sand) was adopted to be compared with substitution levels of 10, 20, 30 and 40%. The higher the mixture lime mud content, the lower the mortars volumetric heat capacity. The ultrasonic pulse velocity was reduced when increasing lime mud and this was attributed to the high porosity of the resulting mortars. The increase in porosity caused by a higher water proportion was also responsible for reductions in thermal conductivity and volumetric heat capacity. Regarding mechanical properties, flexural and compressive strengths were reduced by up to 50 and 59%, respectively. However, mortars up to 20% replacement reached the minimum standardized required strength.

A cement partial replacement by an “as received” and a post-calcination lime mud in mortars produc-

tion was made by (12). Lime mud calcination was carried out at a relatively low temperature, between 650 and 750°C, which represents a lower energy consumption than in ordinary industrial calcination process to obtain lime. Cement partial replacements by lime mud were at levels of 0, 10, 20, 30 and 40% by mass. All produced mortars were tested at compression strength. Compressive strength was satisfactory only for the 10 % non-calcined lime mud mortar (as received lime mud) in relation to reference mortar. As for mortars containing calcined lime mud, compressive strength was satisfactory for replacement levels of up to 30% in relation to reference mortar. The better results of calcined lime mud mortars were attributed to the increased residue reactivity in relation to the non-calcined (as received) residue.

Brazil, favored by its territorial dimension and climatic conditions, has an important position in international market of pulp and paper industry. As a consequence, large volumes of waste are generated every year, reaching more than 15 million tons in 2019 and 128 thousand tons of this volume are lime mud. Furthermore, in paper manufacturing process, it is estimated that for each pulp produced ton, 0.47 m³ of lime mud is generated. Regarding lime, the annual Brazilian production is around 7.8 million tons (13).

These residues are usually disposed of in sanitary landfills, which require large areas. In this way, the potential use of these alkaline residues from pulp and paper industry as raw materials in production of construction materials and components, combined with strict environmental legislation and licensing processes, may represent an interesting alternative for increasing the useful life of landfills, as well as favoring the production of sustainable materials.

In this context, the present work used lime mud, which is widely available in Brazil, for production of multiple-use mortars with reliable properties in civil construction. This work aims to evaluate hydrated lime substitution by lime mud in the manufacture of multiple-use mortars, as well as to verify whether their physical, chemical and mechanical properties are in accordance with standards prescriptions, thus, allowing its reliable application in civil construction.

2. MATERIALS AND METHODS

2.1 Materials

In this work, a limestone blended cement type CP II-F 32, a classification according to Brazilian standard, was used as the main binder for mortars production. According to (14), CP II-F 32 cement has an addition of limestone filler between 6 and 10% and its applications range from reinforced concrete structures to laying and coating mortars. The hydrated lime used in this work can be classified according to (15) as CH-III type, as information provided by the manufacturer. This lime type corresponds to the less pure group in such classification. The purity degree affects both the final price and the performance of the mortar containing this binder since the lower the purity, the cheaper the mortar and the worse its binding properties. The lime mud used in this research was supplied by CENIBRA- The Japanese-Brazilian cellulose company- located in the city of Belo Oriente- MG. Upon receipt, the waste was oven-dried at 100°C for 24 hours. Then, in order to reduce impurities and adjust the particle size to that of hydrated lime, lime mud was sieved through a 75 μm sieve mesh. A river quartz sand (2.24 fine modulus, 2.58 g/cm³ specific mass) was used, as fine aggregate. The sand was first washed on running water to reduce any impurities that might be present after, it was oven-dried at 100°C for 24 hours and finally sieved through a 1.18 mm sieve mesh. Running water was used for all mortar mixes production.

2.2 Methods

The oxide compositions of cement, hydrated lime and lime mud were obtained by energy dispersive X-ray fluorescence spectrometry technique (EDX), using a 3 kW tube and rhodium target EDX-700 spectrometer from Shimadzu. Lime mud and hydrated lime particle size distributions were obtained by laser diffraction technique using a Shimadzu SALD-3101 granulometer. The test was performed under the following conditions: samples dispersed in distilled water, stirring rate at 1500 rpm, 300-second ultrasonic treatment, 19/0 obscuration (19%) and dispersion time of 5 minutes. Mineralogical characterization of raw materials and mortars was performed in a MinFlex 600 (Rigaku) X-ray diffractometer Cu-Kα radiation line (40 kV/ 15 mA), 0.05° step size, 15º/min sweep speed and Bragg angles (2Θ) from 8 to 70°. In order to identify the crystalline phases, a comparison with diffraction peaks of inorganic crystal structures recorded in Rigaku's PDLX 2.0 software database was performed. Lime mud micrographs were obtained using a SUPER-SCAN SSX-550 scanning electron microscope (Shimadzu), working at accelerating voltages of 15 or 20 kV as required, in backscattered electron imaging mode (BSE). Thermogravimetric analysis (TGA) was conducted for lime mud characterization as well as monitoring hydrates formation in mortars. A TGA Q5000 thermogravimetric analyzer (TA Instruments) with a heating rate of 15°C/min from 35°C to 1000°C under an oxygen environment was used.

The real specific mass of raw materials, excepting sand, was determined with the aid of a Le Chatelier volumetric flask, using the procedure defined in (16). This method sets the way in which finely powdered

materials real specific mass is determined, such as cement, plaster, lime, among others. Sand particle size distribution was determined following (17) and its specific mass was determined by the pycnometry.

In this study, the volumetric proportion of 1:1:5 (cement:lime:sand) was adopted for mortars production, because of its great use and because it meets the requirements for small-scale applications. The amount of water needed to achieve a normal consistency (260 ± 5mm) was determined by the cone trunk slump test according to (18) - Table 1. Five different mixtures were prepared according to the standard procedure (18), with different mass substitution levels of hydrated lime by lime mud (LM). Mixtures were named as LM0, LM25, LM50, LM75 and LM100 where the numbers refer to the substitution level expressed in percent.

Table 1. Mortars mix proportions (kg/m³).

Mortar	Cement	Hydrated lime	Lime mud	Sand	Water
LM0	165.9	165.9	0	829.6	215.7
LM25	165.9	124.4	41.5	829.6	215.7
LM50	165.9	82.9	82.9	829.6	215.7
LM75	165.9	41.5	124.4	829.6	215.7
LM100	165.9	0	165.9	829.6	215.7

Once the composition of all five mixtures was determined, cylindrical (50 mm diameter and 100 mm height) specimens were produced in order to identify the mortar with the best mechanical performance at 14 and 28-day axial compression test. Thus, six specimens were produced for each mixture: 03 to be broken at 14 days and 03 to be broken at 28 days. Then, the mechanical strength gain of the best mortar was monitored at the ages of 1, 3, 7, 14, 21, 28 and 60 days after casting, through axial compression and tensile strength by diametrical compression tests (Brazilian test). In this last test, there were also three specimens of each age. After 24 hours pouring, specimens were demolded and stored at laboratory conditions (23 °C and 50% relative humidity) until the test date. In addition, technical feasibility of such mortar was evaluated according to prescriptions in (19).

The axial compression test was conducted in a 1000 kN capacity manual hydraulic press (SOLOTEST) and 0.30 MPa/s of loading speed. In order to ensure the load uniform distribution on the specimen surface during the test, metallic plates coated with neoprene discs were placed on each face of the specimen following (20).

With the purpose of verifying whether the difference between the obtained means was significant, two statistical tests were performed: Dunnett's test and Tukey's test. Thus, the data were submitted to the Shapiro-Wilk test to verify the residuals normality, and the Barlett test to verify the variances homogeneity, at a 5% significance level (21, 22). Once the guesses were confirmed, the variance analysis was performed using the F test at a significance level of 1% probability. After identifying significant differences between at least one of the treatments, means were compared, considering LM0 mortar as a reference treatment. The analysis were carried out with the help of the computational software R, through the RStudio interface (R Core Team, 2020).

After selecting LM100 mortar to continue the research, a detailed analysis of mechanical strength gain was carried out as a function of time, at the ages of 1, 3, 7, 14, 21, 28 and 60 days. For this purpose, axial compression (23) and diametrical compression (24) strength tests were carried out on three 100 mm height and 50 mm diameter cylindrical specimens.

Lime mud effect on mortars hydration kinetics was evaluated by an I-CAL 2000 HPC isothermal calorimeter (Calmetrix). 100 g-mortar samples duplicates were monitored for 48 hours at 23°C.

In order to obtain more characteristics about LM100 mortar, tests prescribed by (19) were carried out. This standard provides the requirements for laying and coating mortars. Such requirements make it possible to classify mortars and evaluate their technological feasibility.

2.2.1. Technological tests at fresh state

The mass density in the fresh state was determined according to (25). To perform this test, a 400 cm³ metal standardized container was used. The standardized metallic container was filled up with 03 approximately equal heights mortar layers, applying 20 strokes in each layer with an upright position spatula. Then, the container was three times dropped on consolidation table. In the end, the container surface was leveled with the aid of a metal ruler and the set mass was measured.

The incorporated air content was determined according to (26). This test uses a metallic cylindrical container filled up with mortar and hermetically closed with a lid, equipped with air valves and taps; the necessary pressure for water injection and exit from the sample was indicated on a manometer. The container was filled up with three layers which were manually compacted with 25 strokes each, using a standard rod. Then, mortar surface was leveled and the lid was placed so that the water was injected into one of the faucets until its exit on the opposite side. Once the taps and valves were closed, the air was injected with the aid of a manual pump until the pressure reached the initially indicated value on manometer, allowing the direct reading of the incorporated air content.

Water retention was determined according to (27). To carry out this test, a modified 200 mm opening Buchner funnel was used coupled to a vacuum pump to make a mortar suction. Initially, a plate containing a moistened filter paper was placed on test funnel to ensure the tightness between them. With the tap closed, the vacuum pump was activated until a 51 mm mercury suction was applied to the system. Then, the tap was turned on for 90 seconds to remove the excess water from filter paper. Subsequently, the plate was filled up with mortar and 16 strokes were evenly applied along the edge. To ensure an homogeneous plate filling 21 strokes were evenly distributed in central region; with movements from center plate to its edge, excess mortar was removed using a metal ruler, until a flat surface was obtained. Then, the suction controlling tap was opened again and a suction was applied to the 51 mm mercury sample for 15 minutes. After this procedure, the dish was removed from the funnel and the set mass was measured.

2.2.2. Technological tests at hardened state

The bulk density test in hardened state followed the methodology of (28). To carry out the test, three 40 mm x 40 mm x 160 mm prismatic specimens were made. The specimens were casted in two layers, each layer was 30 times dropped on consolidation table. After 28 days curing, height, width and length of specimens were measured using a caliper. It is worth mentioning that these measurements were obtained in two or more different positions for each dimension. Then, specimens masses were determined using a 0.1 g precision laboratory balance.

The test to determine capillary water absorption and the mortar capillary coefficient in hardened state was carried out in accordance to (29). This test determines a specimen capillary absorption as a function of mass variation over time, until its stabilization. To carry out this test, three prismatic specimens with dimensions of 40 mm x 40 mm x 160 mm (height, width and length, respectively) were made. The specimens were casted in two layers, each one was 30 times dropped on consolidation table and tested at 28 days.

Specimens surfaces were sanded with a coarse sandpaper (n° 100). Then, a nylon bristles brush was used to clean possible sediments deposited on the surfaces. The initial mass of each specimen was measured and, later, they were placed in a container with water with one of the square cross-section faces supported on its bottom. During the test, the water level was kept constant (5 ± 1 mm) above the water contacting face taking care to avoid wetting the other surfaces. Specimens masses were determined after 10 and 90-minute water contact. Before each weighing, each specimen was previously dried with a damp cloth.

The potential tensile bond strength test was performed in accordance to (30). This test aims to determine the maximum stress achieved in a lining specimen, when subjected to perpendicular tensile stress at a constant loading rate. Initially, a standard concrete substrate was prepared. The substrate was horizontally supported on a flat and firm base. With the aid of a nylon bristles brush, substrate surface was cleaned to remove dust or any other fragment that could impair the mortar-substrate adhesion. A wooden mold with an uniform depth of 18 ± 2 mm was used to place the mortar on substrate. Then, the mortar was pressed against the substrate to eliminate voids and ensure an uniform mortar distribution over the surface. The surface was leveled with a metal ruler and the set was cured in an horizontal position under environment laboratory conditions for 28 days. After 25 days curing, ten 1-mm depth cuts were made in substrate, with the aid of a 50 mm diameter hole saw. Cuts were made with a minimum distance of 20 mm from each other, and distanced from the edge by at least 40 mm. Great care was taken when making the cuts, as they could interfere with the coating integrity. After cutting the coating, ten 50 mm diameter metallic inserts were glued using epoxy resin in the area delimited by the cuts. At 28 days, the test was performed by applying a perpendicular traction effort, using a SOLOTEST brand equipment.

The flexural tensile strength and compressive strength tests were performed in accordance to (31). To carry out these tests, three 40 mm x 40 mm x 160 mm prismatic specimens were tested at 28 days using an universal test machine (5582 Machine, Instron), with a servomechanical drive system, 100-kN maximum capacity, and displacement rate of 0.5 mm/min. To determine the tensile strength in bending, the three-point bending tensile test was used. Thus, the specimen was placed with its ends resting on the device with a free span of 110 mm and a constant load speed of 50 ± 10 N/s which was applied at its geometric center, until failure. The specimen failure in bending happens practically in the middle of the free span, that is, the specimen is half divided. These halves were used to determine the compressive strength. In this way, the new specimen was placed between two metallic supports and a constant load speed of 500 ± 50 N/s was applied until failure.

3. RESULTS AND DISCUSSION

3.1 Materials characterization

Figure 1 compares the particle size distribution curves of hydrated lime and lime mud. Scanning electron microscopy analysis is an analytical tech-

nique that allows identifying morphological characteristics of solid materials. In general, lime mud microstructure is composed of cubic crystalline particles (Figure 2) a calcite characteristic (9), which was confirmed in the X-ray diffraction analysis (Figure 3).

X-ray diffraction allows the verification of the crystalline phases of materials. According to this technique, the only crystalline phase identified in lime mud was calcite ($CaCO_3$), as shown in Figure 3. The thermogravimetric (TG) curve of lime mud and its differential (DTG) is shown in Figure 4. An endothermic peak at approximately 730°C is

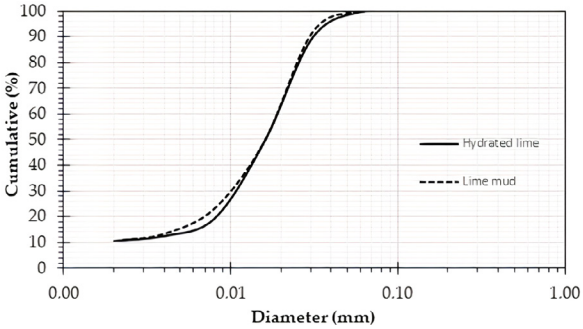

FIGURE 1. Particle size distribution by laser diffraction of hydrated lime and lime mud.

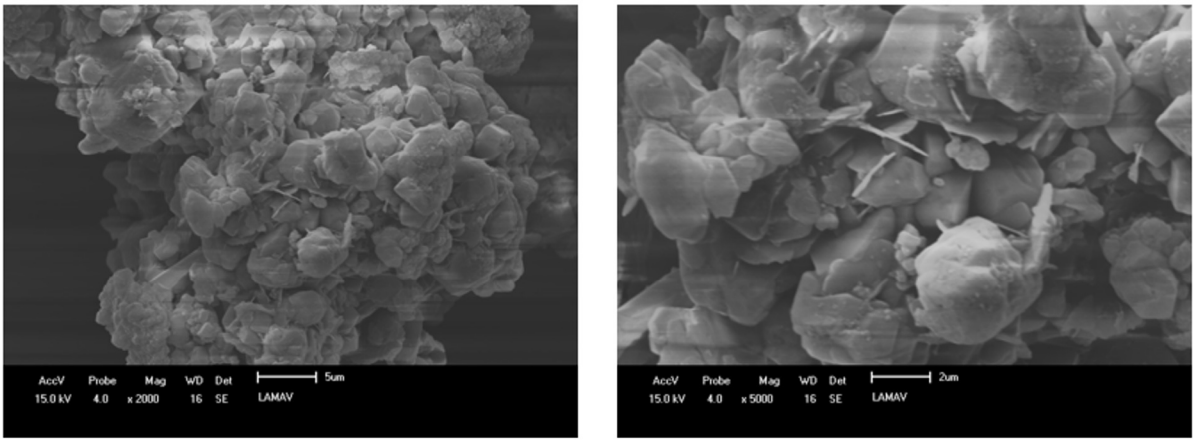

(a) (b)

FIGURE 2. Lime mud micrographs: a) 2000x magnification; b) 5000x magnification.

observed along with a mass loss of approximately 42%. This phenomenon is related to the CO_2 output during sample heating, resulting from the decomposition reaction of calcium carbonate existing in lime mud (Figure 3), as shown in Equation [1]:

$$CaCO_3 \rightarrow CaO + CO_2 \qquad [1]$$

Table 2 shows the real specific mass of CP II-F 32 cement, CH-III hydrated lime and lime mud.

Table 3 shows the chemical composition of the raw materials. It is noticed that the CaO percentage present in lime mud is slightly higher than that of hydrated lime. It is observed that lime mud is composed of approximately 98% of CaO, related to the causticizing process in the white liquor chemical recovery phase. However, it is noteworthy that the CaO identified in lime mud is related to $CaCO_3$. In

TABLE 2. Real specific mass of raw materials.

Real specific mass (g/cm³)		
CP II-F 32	CH-III	Lime mud
2.99	2.69	2.64

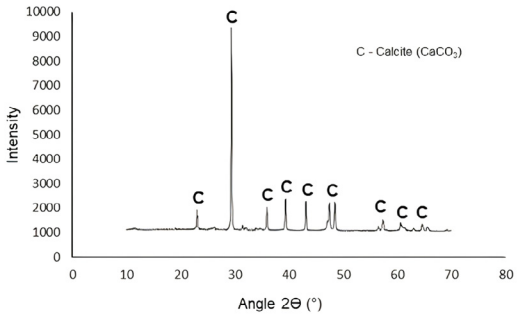

FIGURE 3. X-ray diffractogram of lime mud.

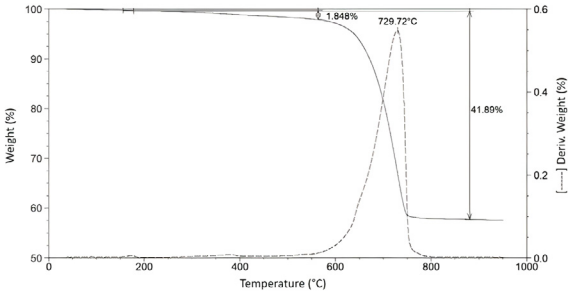

FIGURE 4. TG and DTG of lime mud.

hydrated lime, the indicated CaO is present in the form of $Ca(OH)_2$. The other oxides, identified in smaller amounts, are leftovers from chemical pulping process.

It is also noteworthy that the name of the residue studied in this research induces to an erroneous association with reactive lime, when, in fact, lime mud is predominantly formed by limestone itself, that is, an inert material. This behavior was confirmed when analyzing the pozzolanic activity index (IAP) of lime mud according to (32). The value found was 57%, which indicates low amorphous or reactive content. To be considered a pozzolanic material, this value must reach at least 75%, according to the requirements prescribed in (33).

TABLE 3. Chemical composition of raw materials (% by mass).

Oxide	CP II-F 32	CH-III	Lime mud
CaO	82.740	95.520	97.787
Fe_2O_3	2.933	-	0.049
K_2O	0.564	1.209	1.295
SrO	0.171	0.037	0.205
ZrO_2	0.017	-	0.008
SO_3	2.683	0.636	0.656
SiO_2	10.471	2.597	-
MnO	0.103	-	-
TiO_2	0.317	-	-

3.2. Determination of the optimal proportion

Figure 5 shows the mean compressive strength values of evaluated mortars at 14 and 28 days. It can be observed that LM100 mortar has reached the best mechanical performance (4.6 MPa) at 14 days. However, at 28 days, LM25 mortar has showed the highest compressive strength, reaching 6.4 MPa.

The obtained results were first statistically analyzed by the Dunnett's test. This test is suitable to compare a reference treatment with other treatments, when there is no interest in comparing the other treatments among themselves (34). That is, each treatment is compared separately with the control treatment.

At 14 days, the compressive strengths of LM0, LM25, LM50 and LM75 mortars have showed no significant differences among each of them. In addition, it should be noted that the LM100 mortar average was the highest among the other treatments average.

Statistical analysis of the 28 results has showed that LM0, LM50, LM75 and LM100 mortars compressive strengths are equivalent. Furthermore, LM25 mortar average was the highest among the other treatments average. Therefore, it is concluded

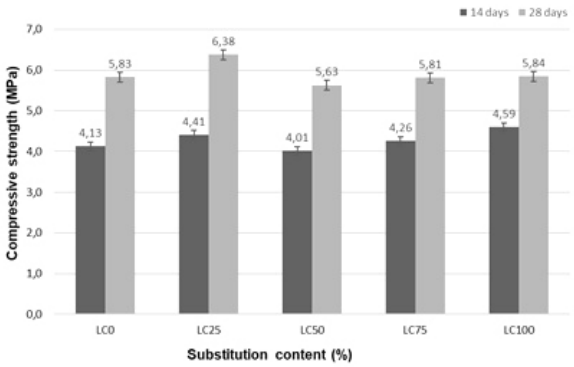

FIGURE 5. Compressive strength at 14 and 28 days.

that the partial or total replacement of hydrated lime by lime mud did not compromise the final product compressive strength, on the contrary, the strength has increased or remained unchanged in comparison to the reference mix without any substitution.

The second statistical analysis performed on compressive strength results was the Tukey test. This test uses the same assumptions as the Dunnett's test. However, the Tukey test is considered more refined, as it compares the average of all treatments against each other, unlike the Dunnett's test, which only compares the averages only with a reference treatment (35). At 14 days, the average values of LM25, LM75 and LM100 mortars were statistically equal to each other. On the other hand, LM100 mortar average was higher than that of LM0 and LM50 mortars.

Finally, results of compressive strength at 28 days showed that the average values of LM0, LM50, LM75 and LM100 mortars were statistically equal and all of them were lower than the LM25 mortar.

Although LM25 mortar has reached the highest 28-day compressive strength among all others, based on results obtained through the two statistical tests, LM100 mortar represents a product with higher practical interest compared to the other mixtures, since it was possible to replace 100% of hydrated lime by lime mud without compromising the final product mechanical strength. It's also noteworthy that it's still obtaining the best environmental/sustainable result, since it reduces the need for limestone extraction and calcination, in order to produce hydrated lime for Civil Construction.

Thus, LC100 mortar was chosen to continue this research. From that moment on, due to the small amount of available material and time, the other tests were only performed on reference mortar and LC100 mortar, so that results could be compared. Therefore, intermediate mortars results could not be obtained.

Furthermore, it is noteworthy that mortars compressive strength values were similar even with different replacement contents, as the filling effect provided by the residue (filler effect) contributed in a similar way to the hydrated lime reactivity.

3.3. LM100 mortar mechanical strength development

Figure 6 shows the LM100 mortar mechanical strength gain over time. Regarding the axial compressive strength, the most accentuated gain in strength is observed, which occurs up to the seventh day, followed by a relatively uniform increase up to the 28th day. At the third and seventh day, the mortar has reached an axial compressive strength of 50 and 68%, respectively, in relation to that recorded at 28 days.

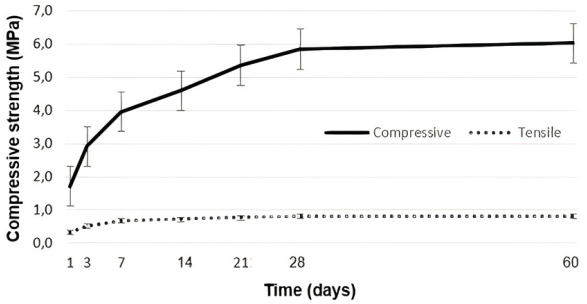

FIGURE 6. LM100 mechanical strength development as a function of time.

Regarding the tensile strength by diametral compression test, there was a more expressive increase up to 14 days. Just as compressive strength, from 28 days onwards the strength value remained practically unchanged, showing again that the maximum strength is reached at this age. At 28 days, the tensile strength by diametrical compression has reached 0.8 MPa, which represents approximately 14% of compressive strength at that same age.

3.4. Technological tests at fresh state

Table 4 shows the results of the technological tests at fresh and hardened states, as well as their respective classifications according to (19). It can be seen that the replacement of hydrated lime by lime mud has resulted in a small decrease (2%) in mortar mass density at fresh state, but it does not represent significant losses in this property. This is in accordance to Table 2, since hydrated lime CH-III has a little bigger density than that of lime mud.

Also according to Table 4, both LM0 mortar and LM100 mortar are classified as D6. From a mechanical point of view, this is a positive characteristic, as this class mortars have a high mass density at fresh state, which suggests a grains adequate packing and, consequently, a low void index. On the other hand, low-density values may indicate a lot of trapped air inside the mortar, affecting the final product mechanical strength.

TABLE 4. Technological tests at fresh and hardened states (19).

Testing	Result		Unit	Classification	
	LM0	LM100		LM0	LM100
At fresh state					
Mass density at the fresh state	2047	2004	kg/m³	D6	D6
Entrained air content	8	10	%	-	-
Water retention	94	98	%	U5	U6
At hardened state					
Bulk density in hardened state	1870	1800	kg/m³	M5	M5
Capillary water absorption	13.13	16.51	g/dm²·min$^{1/2}$	C6	C6
Potential tensile adhesion strength	0.25	0.16	MPa	A2	A1
Flexural tensile strength	1.65	1.53	MPa	R3	R3
Compressive strength	6.83	6.11	MPa	P5	P5

Note that the total replacement of hydrated lime by lime mud in mortar caused a small increase of 2% in the entrained air content. The Brazilian Association of Portland Cement (ABCP) recommends an incorporated air content between 7 and 17% to ensure adequate conditions in mortar application. Therefore, it is observed that both LM0 and LM100 mortars present values within the recommended range.

According to (36), both entrained air content and water retention are properties that directly influence the workability and, consequently, the feasibility of these mortars use. Excessive entrained air could cause durability problems in cementitious materials due to the matrix high porosity, allowing an easier entry of CO_2, as well as other aggressive agents, if these pores are interconnected. These gases may react with the cementitious paste and cause an weakening to the final product (37).

According to Table 4, LM100 mortar is classified as U6, indicating high water retention capacity. It can be observed that the replacement of hydrated lime by lime mud caused an increase of 4% in the mortar water retention. (9) obtained a 3.6% increase

in water retention by replacing 10% of CH-III with the primary sludge from pulp and paper industry. This increase was attributed to the presence of cellulose in the residue, as this material can lead to formation of reactive components that favor water retention (38).

This characteristic is favorable, because the greater the water retention, the better the application condition. The presence of water allows mortar hardening reactions to be more gradual, promoting proper cement hydration and consequently material strength gain. Otherwise, the rapid water loss from mortar to the substrate, over which it will be applied, may cause material small cracks, compromising its mechanical strength and the wall aesthetic appearance (39).

3.5. Technological tests at hardened state

According to Table 4, it is verified that both LM0 mortar and LM100 mortar are classified as M5, having high bulk density at hardened state. Reductions in hardened mass density in relation to fresh mass density for LM0 and LM100 mortars were approximately 9% and 10%, respectively. These differences are mainly explained by the water loss due to drying during specimens curing.

According to (40), Portland cement-based mortars have their density reduced from 3 to 11% when cured at room temperature. Thus, it is noted that both mortars were within the limits of conventional mortars.

When evaluating the influence of partial cement substitution by lime mud in self-compacting mortars for floors, (10) found that bulk density at hardened state tended to decrease when increasing lime mud content. However, an inverse behavior was observed for porosity.

According to Table 4, both LM0 and LM100 mortars are classified as C6, indicating high permeability. This characteristic is not very suitable for coating mortars, as permeability is related to material susceptibility to degradation. (41) demonstrated that mortars with capillary coefficients above 35 $g/dm^2 \cdot min^{1/2}$ have their performance impaired at the medium and long term, which is not therefore, the case obtained in this study.

A porous material is more permeable, but it is noteworthy that for this material to be permeable there must be an interconnection between the pores. Therefore, it can be concluded that all permeable material is porous, but not all porous material is permeable (42). There is a direct relationship between permeability and porosity. Thus, it is observed that LM100 mortar is a little more permeable than LM0 and, consequently, more porous.

There was a significant drop in mass density at hardened state compared to fresh state in LM100 mortar. As LM100 mix has showed high water retention, during the drying process, this water evaporates, creating interconnected voids in matrix. This explains the high capillarity coefficient found. Although it is a porous material, the compressive and tensile strength values are acceptable. It is noteworthy that porosity and mechanical strength are inversely proportional quantities, the greater the porosity, the lower the mechanical strength (43).

According to Table 4, LM0 mortar is classified as A2, indicating good adhesion to substrate, and LM100 as A1, that is, low adhesion to substrate. Therefore, it is observed that when replacing hydrated lime by lime mud, mortar-substrate adhesion decreases, since the porosity of LM100 is greater than that of LM0, with, consequently, a reduction in contact area for stresses transfer between mortar and substrate.

According to Table 4, LC0 mortar is classified as A2, indicating good adhesion to substrate, and LC100 as A1, or poor adhesion to substrate. Therefore, note that LC100 porosity is greater than that of LC0, decreasing, consequently, the contact area for training download mechanics between mortar and substrate.

According to (44), adhesion is a very important property in coating mortars, as it is related to the ability of the coating to remain adhered to substrate when tensions arise at the substrate-coating interface. In addition, inadequate conditions at mortar-substrate interface allow pathological manifestations, such as detachment/fall of facade plates. Therefore, the greater the mortar-substrate adhesion, the better the performance of the constructive system.

Regarding the type of rupture, 80% of LM100 specimens evaluated by the adhesion test showed the rupture at the substrate/mortar interface (Figure 7a) while the rest happened directly in the mortar (Figure 7b), confirming in the latter the low adhesion of the mortar to the substrate. As for the LM0 mortar, the rupture was in the mortar in all specimens, confirming that this one has better adhesion than that one.

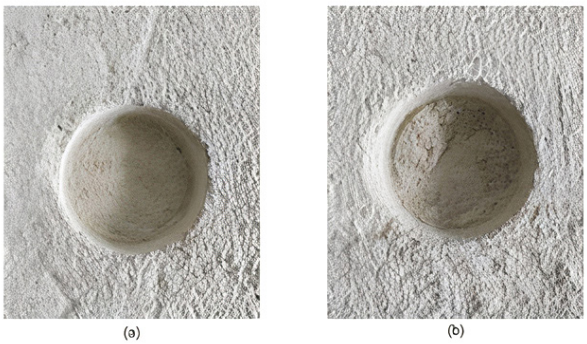

FIGURE 7. Rupture types in the tensile adhesion test: (a) a rupture in the mortar; (b) a rupture at the mortar-substrate interface.

According to Table 4, it is observed that both mortars are classified as R3 for tensile strength and as P5 for compressive strength. For LM100 mortar, tensile strength result (1.53 MPa) corresponds to 25% of compressive strength (6.11 MPa), at 28 days. For LM0 mortar, this ratio was 24% at the same age.

Note that tensile and compressive strength values for LM0 mortar were a little higher than these of LM100 mortar. This difference is related to materials porosity, since LM100 mortar is more porous than LM0, as shown above.

The values obtained in this study for tensile and compressive strength were consistent with those reported by (45) and (46). On the other hand, current results were lower than those reported by (12) who partially replaced Portland cement by a 750 ° C calcined sludge, a treatment that increased the residue reactivity.

According to (47), tensile and compressive strength are not the main properties in coating mortars. In this case, workability and adhesion are more relevant. (48) stated that, in bricks and blocks laying, especially in structural masonry, the mortar compressive strength should not be much lower than that of the blocks, so as not to compromise the final strength of the constructive system.

3.6. Analytical tests

Figure 8 compares thermogravimetry results of LM0 and LM100 mortars. It can be noticed a very similar behavior between the mortars. The first peak in the DTG curve, between 50 and 100°C, represents the loss of free, adsorbed or capillary water and is proportional to the amount of water present in mortar pores. The second peak, around 130°C, is related to C-S-H (49). The third peak at 435.39°C in LM0 and 444.32°C in LM100 is attributed to the portlandite dihydroxylation (Equation [2]). In addition, up to this peak, a mass loss of 3.9% in LM100 and 4.6% in LM0 is observed.

$$Ca(OH)_2 \rightarrow \mathrm{CaO} + H_2O \qquad [2]$$

The fourth and last peak is the most expressive and is related to the calcite and dolomite decomposition (Equations [1] and [3]), which occurs at approximately 750°C, demonstrating that samples underwent carbonation (50). As thermogravimetric analysis was performed with a heating rate of 15°C/min (relatively fast), it was not possible to differentiate the peaks in which calcite and dolomite decompositions occur. Probably, if the test had been done with a slower heating rate (5°C/min or less), for example, decompositions could have been identified with better accuracy.

$$CaMg(CO_3)_2 \rightarrow \mathrm{CaO} + \mathrm{MgO} + 2CO_2 \qquad [3]$$

Note that, although LM0 mortar has a slightly higher amount of portlandite and a lower amount of calcium carbonate compared to LM100, this difference was not enough to significantly change the 28-day mortars compressive strength, as it was compensated by the amount of CSH slightly higher in LM0. It is noteworthy that C-S-H was identified in thermal analysis, as it has a semi-crystalline to amorphous structure and thermogravimetry enables the identification of glassy phases. Therefore, this analytical technique complements the results obtained by X-ray diffraction (XRD).

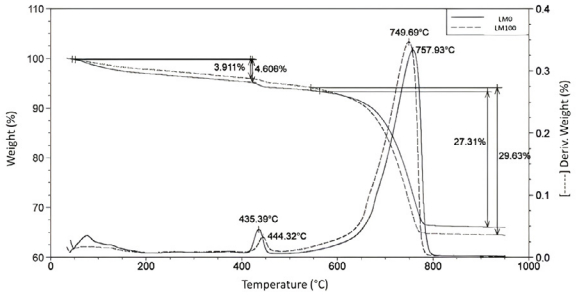

FIGURE 8. TG and DTG curve of LM0 and LM100 mortars.

Thermogravimetric curves of the other mortars are shown in Figures 9 to 11. When comparing all mortars, it is noted that LM100 had the lowest mass loss until portlandite dihydroxylation (3.9%) and that all mortars had similar total mass losses.

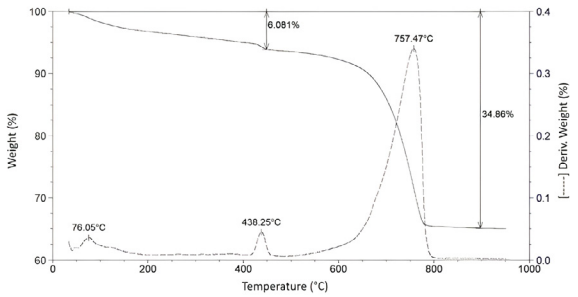

FIGURE 9. TG and DTG curve of LM25 mortar.

LM0 was the mortar with the lowest total mass loss (33.6%). On the other hand, the one with the highest total mass loss was LM75 (35.68%). This small difference may be explained by the presence of organic matter in lime mud, as it is a residue from cellulosic pulp production (a plant origin material) and which has not undergone any previous processing (calcination, for example), unlike hydrated lime, which comes from a mineral extraction process with subsequent calcination.

Figure 12 compares the diffractograms of the five studied mortars. Crystalline phases identified in samples were: calcite ($CaCO_3$), dolomite [$CaMg(CO_3)_2$],

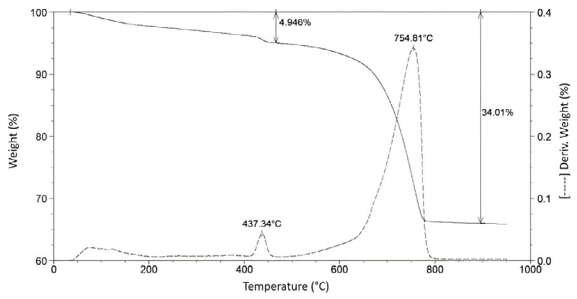

FIGURE 10. TG and DTG curve of LM50 mortar.

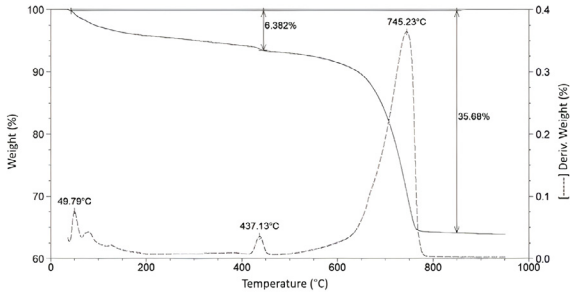

FIGURE 11. TG and DTG curve of LM75 mortar.

portlandite [$Ca(OH)_2$] and silica (SiO_2), represented in the diffractogram by C, D, CH and Q, respectively. Peaks intensity is related to the greater or lesser amount of a certain crystalline phase present in sample.

Comparing the samples, the main difference observed was the gradual reduction in dolomite amount as hydrated lime was replaced by lime mud. This result indicates that hydrated lime contains more Mg^{2+} in its composition than lime mud. Although Mg^{2+} was not identified in X-ray fluorescence analysis - EDX, this element was identified in XRD analysis, as this analytical technique is more sensitive than that (51).

In relation to the other crystalline phases, it is noted that peaks remained practically unchanged for all samples. These results justify the very close mechanical strength values of the evaluated mortars (Figure 7).

Figures 13 to 15 show the heat flux curves of LM0 and LM100 mortars obtained by isothermal calorimetry at 23°C. The calorimetric behavior of the two mortars was very similar, so that the heat flux curves of both, when inserted in the same graph, were practically overlay. So, to better observe the main differences between them, we chose to insert the curves side by side (Figure 13) and overlay on a smaller scale with emphasis on the main peaks (Figures 14 and 15).

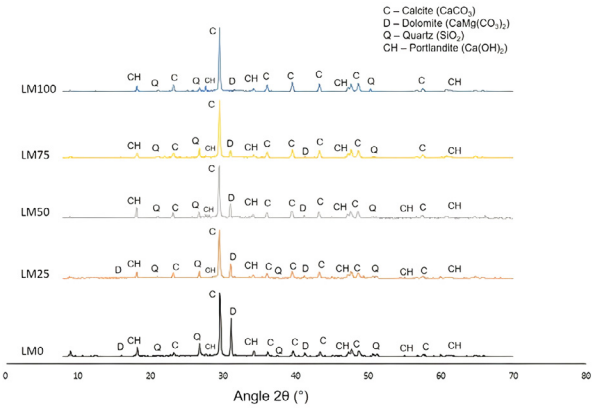

FIGURE 12. Mortars X-ray diffractograms.

During the first few minutes, a certain amount of heat is released due to binder particles hydration and crystals dissolution (stage I). Then, begins the period of hydration by induction, in which a higher ions concentration is reached, as particles continue to dissolve and crystalline hydrates are formed (stage II). After induction period, cement hydrates crystallize (stage III). Then the heat release and processes slow down (stages IV and V).

Figure 14 shows the initial peak of LM0 and LM100 mortars heat flux curves. Test time starts to be counted from the moment the binder are exposed

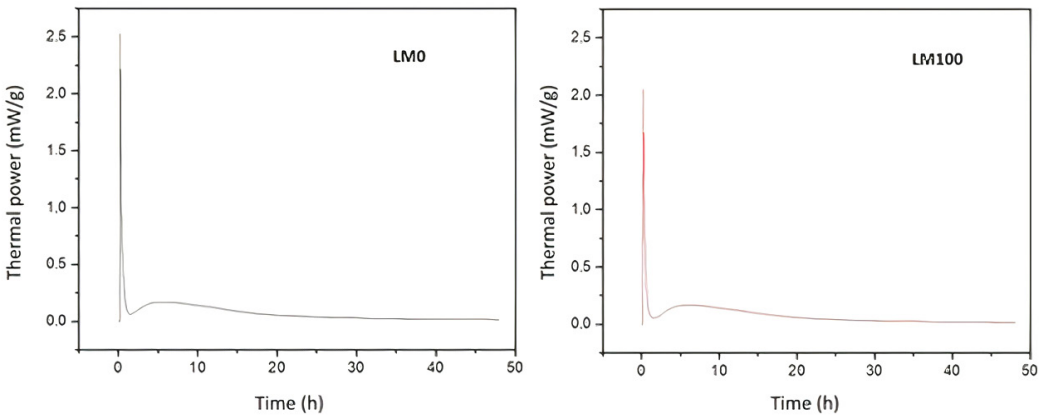

FIGURE 13. Heat flux of LM0 and LM100 mortars.

to water, so the graph does not start at zero time. In the present study, time taken from mortar preparing to placing samples in the equipment was approximately 8 minutes.

During stage I of hydration, the total replacement of hydrated lime by lime mud did not significantly affect the heat release rate. (52) also observed this behavior by partially replacing Portland cement by lime mud dried at 75°C. Note that LM0 mortar maximum thermal energy value was 2.5 mW/g and that of LM100 mortar was 2.0 mW/g.

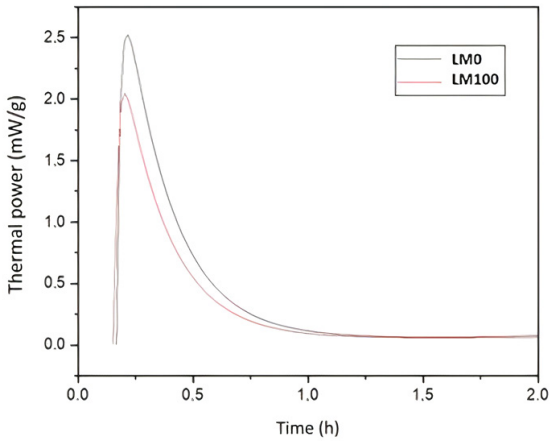

FIGURE 14. Stage I of hydration of LM0 and LM100 mortars.

Figure 15 shows the induction (stage II) and acceleration (stage III) periods of LM0 and LM100 mortars. It is observed that in LM100 mortar the hydration by induction period is a little longer and causes a slight delay in heat release at stage III. Thus, setting time is delayed by approximately 15 minutes compared to LM0. It is also noted that in LM0 mortar the setting start and end times occur in 2 and 4 hours, respectively. In LM100 mortar, these times occur in 2.25 and 4.25 hours.

According to (53), setting is defined as the cement paste stiffening when passing from a fluid to a rigid state, being a physical consequence of the chemical processes that occur inside the paste. The pick start time marks the point at which the paste is no longer workable. The end of setting time represents the time required for the paste to completely solidify. Therefore, it is noted that LM100 mortar may be workable for a longer period of time than LM0 mortar (approximately 0.25 hours or 15 minutes).

In addition to heat flux curves, by integrating the obtained data from the calorimeter, according to the procedure described in ASTM C1702, curves of total released heat or accumulated hydration heat up to 48 hours were obtained (Figure 16). The amount of released heat in LM0 mortar was 131 J/g and in LM100 it was 128.1 J/g. Note that when completely replacing hydrated lime by lime mud, the amount of released heat decreased by about 3%.

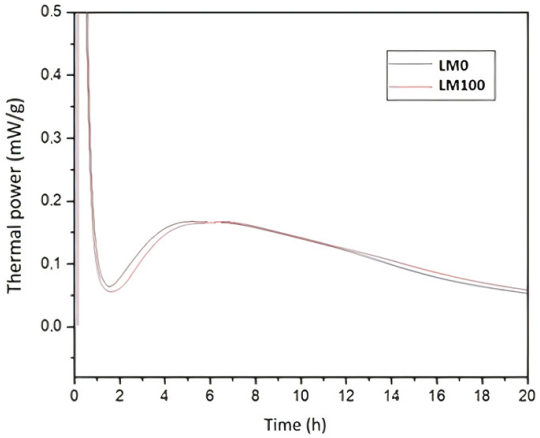

FIGURE 15. Stages II and III of LM0 and LM100 mortars hydration.

According to (53), hydration heat may be favorable in certain situations, for example, when providing activation energy for hydration reactions in cold places, and unfavorable in others, for example, in large volume structures structural cracking. The greater the hydration heat, the greater the thermal retraction and, consequently, the greater the cracks appearance. Thus, in addition to the aesthetic factor, cracking compromises the durability of structural elements, as it allows the entry of aggressive agents that cause destructive chemical reactions, such as carbonation and acids and sulfates attack.

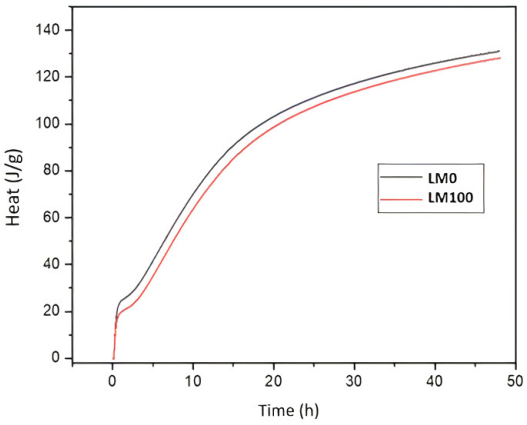

FIGURE 16. Hydration heat of LM0 and LM100 mortars.

The mortars micrographs were taken by SEM observations after 28 days curing at room temperature in the laboratory. Figures 17 and 18 show LM0 and LM100 mortars micrographs, respectively. According to these images, both mixes do not have significant differences in their microstructures features and that is consistent with their similar mechanical strength results.

The indicated points in Figures 17-b and 18-b show the formation of acicular-shaped ettringite crystals (Spot 1), calcite crystals (Spot 2), hexagonal sheets of portlandite (Spot 3) and CSH (Spot 4)

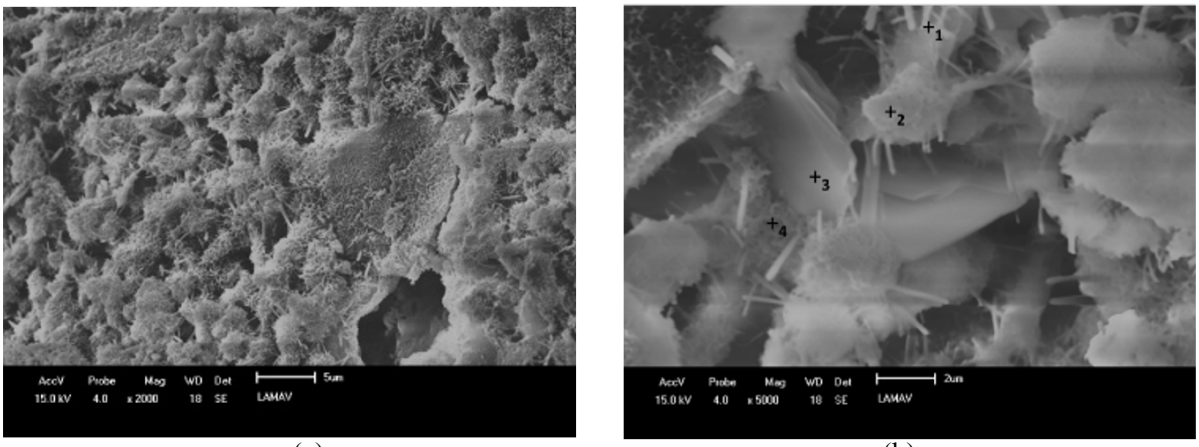

(a) (b)

FIGURE 17. LM0 mortar micrograph with a) 2000x and b) 5000x magnification.

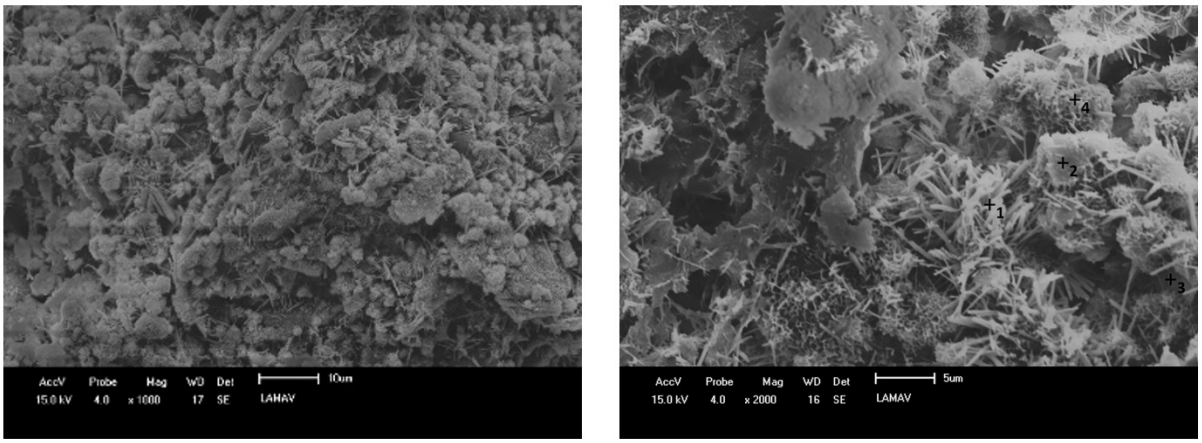

(a) (b)

FIGURE 18. LM100 mortar micrograph with a) 1000x and b) 2000x magnification.

in both mortars, mineral phases which are responsible for mechanical strength. Such phases were also identified by (36) when evaluating the influence of primary sludge from pulp and paper production on the properties of Portland cement pastes and mortars and by (52) when analyzing the influence of lime mud dried at 75°C on cement hydration.

Microstructural characteristics are consistent with thermogravimetric analysis, which have indicated a lower presence of portlandite in LM100 mortar compared to LM0, and this phase is less apparent in micrographs, while calcite is widely observed in both mortars.

4. CONCLUSIONS

Based on the results obtained in experimental program, the following conclusions can be drawn:

- The chemical composition of lime mud has indicated that the residue is predominantly composed of CaO present in form of $CaCO_3$, that is, lime mud is practically a limestone;
- Replacing hydrated lime by lime mud in mortars production maintains the water demand for the normal consistency level;
- No significant difference was observed among mortars compressive strengths, despite the replacement rate, except at 25% substitution that was slightly higher at 28 days, because the filler effect provided by the residue contributed in a similar way to hydrated lime reactivity;
- Besides, a similar response in terms of mass density at fresh and hardened states, entrained air content and water retention was found in all mixes regardless substitution level of hydrated lime by lime mud;
- However, capillarity coefficient and adhesion capacity to substrate were negatively affected

when hydrated lime was totally replaced by lime mud (LM100 mortar), as both parameters are quite dependent on a pores structure development;
- Results from TGA, XRD, isothermal calorimetry and micrographs observations by SEM showed similar microstructure features for both plain lime mud composition (LM100) and reference mix (LM0), which can confirm their close results in terms of mechanical behavior;

Finally, it is concluded that it is possible to replace hydrated lime by lime mud in multiple-use mortars production and obtain a material with satisfactory characteristics for Civil Construction applications.

AUTHOR CONTRIBUITIONS:

Conceptualization: H.S. Gonçalves, D.P. Dias, R.C. Lara. Data curation: H.S. Gonçalves. Formal analysis: H.S. Gonçalves. Funding acquisition: D.P. Dias, R.C. Lara. Investigation: H.S. Gonçalves. Methodology: H.S. Gonçalves. Project administration: D.P. Dias, R.C. Lara. Resources: D.P. Dias. Software: H.S. Gonçalves, R.C. Lara. Supervision: D.P. Dias, R.C. Lara. Validation: H.S. Gonçalves, D.P. Dias, R.C. Lara. Visualization: H.S. Gonçalves, D.P. Dias, R.C. Lara. Writing, original draft: H.S. Gonçalves, D.P. Dias, R.C. Lara. Writing, review & editing: H.S. Gonçalves, D.P. Dias, R.C. Lara.

AKNOWLEDGEMENTS

Funding: This study was financed in part by the Coordenação de Aperfeiçoamento de Pessoal de Nível Superior – Brasil (CAPES) – Finance Code 001.

REFERENCES

1. Deus, R.M.; Battistelle, R.A.G.; Silva, G.H.R. (2017) Current and future environmental impact of household solid waste management scenarios for a region of Brazil: carbon dioxide and energy analysis. *J. Clean. Prod.* 155 [1], 218-228. https://doi.org/10.1016/j.jclepro.2016.05.158.
2. Fetene, Y.; Addis, T.; Beyene, A.; Kloos, H. (2018) Valorisation of solid waste as key opportunity for green city development in the growing urban areas of the developing world. *J. Environ. Chem. Eng.* 6 [6], 7144–7151. https://doi.org/10.1016/j.jece.2018.11.023.
3. Mymrin, V.A.; Alekseev, K.P.; Catai, R.E.; Izzo, R.L.S.; Rose, J.L.; Nagalli, A.; Romano, C.A. (2015) Construction material from construction and demolition debris and lime production wastes. *Construct. Build. Mater.* 79, 207-213. https://doi.org/10.1016/j.conbuildmat.2015.01.054.
4. Contreras, M.; Teixeira, S.R.; Lucas, M.C.; Lima, L.C.N.; Cardoso, D.S.L.; Da Silva, G.A.C.; Gregorio, G.C.; De Souza, A.E.; dos Santos, A. (2016) Recycling of construction and demolition waste for producing new construction material (Brazil case-study). *Construct. Build. Mater.* 123, 594-600. https://doi.org/10.1016/j.conbuildmat.2016.07.044.
5. Alves, E.D.; Pinheiro, O.S.; Costa, A.O.S.; Junior, E.F.C. (2015) Study of the Kraft pulp obtaining process with emphasis on the lime kiln. Liberato, *Novo Hamburgo.* 16, 205-217.
6. Goel, G.; Kalamdhad, A.S. (2017) An investigation on use of paper mill sludge in brick manufacturing. *Constr. Build. Mater.* 148, 334-343. https://doi.org/10.1016/j.conbuildmat.2017.05.087.
7. Novais, R.M.; Carvalheiras, J.; Senff, L.; Labrincha, J.A. (2018) Upcycling unexplored dregs and biomass fly ash from the paper and pulp industry in the production of eco-friendly geopolymer mortars: A preliminary assessment. *Constr. Build. Mater.* 184, 464–472. https://doi.org/10.1016/j.conbuildmat.2018.07.017.
8. Bui, N.K.; Satomi, T.; Takahashi, H. (2019) Influence of industrial by-products and waste paper sludge ash on properties of recycled aggregate concrete. *J. Clean. Prod*. 214, 403-418. https://doi.org/10.1016/j.jclepro.2018.12.325.
9. Mymrin, V.; Pedroso, C.L.; Pedroso, D.E.; Avanci, M.A.; Meyer, S.A.; Rolim, P.H.B.; Argenta, M.A.; Ponte, M.J.J.; Gonçalves, A.J. (2020) Efficient application of cellulose Pulp and paper production wastes to produce sustainable construction materials. *Constr. Build. Mater.* 263, 120604. https://doi.org/10.1016/j.conbuildmat.2020.120604.
10. Borinaga-Treviño, R.; Cuadrado, J.; Canales, J.; Rojí, E. (2021) Lime mud waste from the paper industry as a partial replacement of cement in mortars used on radiant floor heating systems. *J. Build. Engineer*. 41, 102408. https://doi.org/10.1016/j.jobe.2021.102408.
11. Modolo, R.C.E.; Senff, L.; Labrincha, J.A.; Ferreira, V.M.; Tarelho, L.A.C. (2014) Lime mud from cellulose industry as raw material in cement mortars. *Mater. Construcc.* 64 [316], e033. https://doi.org/10.3989/mc.2014.00214.
12. Vashistha, P.; Kumar, V. (2020) Paper mill lime sludge valorization as partial substitution of cement in mortar. Emerging technologies for waste valorization and environmental protection. Springer, Singapore.
13. IBÁ - Brazilian Tree Industry. (2020) Annual report**.** 66 p. Retrieved from: https://iba.org/datafiles/publicacoes/relatorios/relatorio-iba-2020.pdf. Accessed on: April 20, 2021.
14. NBR 16697. (2018) NBR 16697 - Portland cement – Requirements. Brazilian Association of Technical Norms. Rio de Janeiro. Brazil (In Portuguese).
15. NBR 7175. (2003) NBR 7175 - Hydrated lime for mortar – Requirements. Brazilian Association of Technical Norms. Rio de Janeiro. Brazil (In Portuguese).
16. NBR NM 23. (2000) NBR NM 23 - Portland cement - density determination. Brazilian Association of Technical Norms. Rio de Janeiro. Brazil (In Portuguese).
17. NBR NM 248. (2003) NBR NM 248 - Aggregates - Determination of particle size composition. Brazilian Association of Technical Norms. Rio de Janeiro. Brazil (In Portuguese).
18. NBR 13276. (2016) NBR 13276 - Mortars applied on walls and ceilings - Determination of the consistence index. Brazilian Association of Technical Norms. Rio de Janeiro. Brazil (In Portuguese).
19. NBR 13281. (2005) NBR 13281 - Mortar for laying and coating walls and ceilings – Requirements. Brazilian Association of Technical Norms. Rio de Janeiro. Brazil (In Portuguese).
20. ASTM C1231. (2000) Standard practice for use of unbounded caps in determination of compressive strength of hardened concrete cylinders. American Society for Testing and Materials. Novo México.
21. Shapiro, S.S.; Wilk, M.B. (1965) An analysis of variance test for normality (complete sample). *Biometrika*. 52 [3], 591-611. https://doi.org/10.2307/2333709.
22. Barlett, M.S. (1937) Properties of sufficiency and statistical tests. *Proc. Royal Statis. Soc. – Serie A*. 60, 268-282. https://doi.org/10.1098/rspa.1937.0109.
23. NBR 5739. (2018) NBR 5739 - Concrete - Compression tests of cylindrical specimens. Brazilian Association of Technical Norms. Rio de Janeiro. Brazil (In Portuguese).
24. NBR 7222. (2011) NBR 7222 - Concrete and mortar - Determination of tensile strength by diametrical compression of cylindrical specimens. Brazilian Association of Technical Norms. Rio de Janeiro. Brazil (In Portuguese).
25. NBR 13278. (2005) NBR 13278 - Mortar for laying and coating walls and ceilings - Determination of mass density and incorporated air content. Brazilian Association of Technical Norms. Rio de Janeiro. Brasil (In Portuguese).

26. NBR NM 47. (2002) NBR NM 47 - Concrete - Determination of air content in freshly mixed concrete - Pressure method. Brazilian Association of Technical Norms. Rio de Janeiro. Brasil (In Portuguese).
27. NBR 13277. (2005). NBR 13277 - Mortars applied on walls and ceilings - Determination of the water retentively. Brazilian Association of Technical Norms. Rio de Janeiro. Brazil. (In Portuguese).
28. NBR 13280. (2005) NBR 13280 - Mortar for laying and coating walls and ceilings - Determination of bulk density in hardened state. Brazilian Association of Technical Norms. Rio de Janeiro. Brazil. (In Portuguese).
29. NBR 15259. (2005) NBR 15259 - Mortars applied on walls and ceilings - Determination of water absorption coefficient due to capillary action. Brazilian Association of Technical Norms. Rio de Janeiro. Brazil. (In Portuguese).
30. NBR 13528. (2010) NBR 13528 - Coating of inorganic mortar walls and ceilings - Determination of tensile bond strength. Brazilian Association of Technical Norms. Rio de Janeiro. Brazil. (In Portuguese).
31. NBR 13279. (2005) NBR 13279 - Mortars applied on walls and ceilings - Determination of the flexural and the compressive strength in the hardened stage. Brazilian Association of Technical Norms. Rio de Janeiro. Brazil. (In Portuguese).
32. NBR 5752. (2014). NBR 5752 - Pozzolanic materials - Determination of performance index with Portland cement at 28 days. Brazilian Association of Technical Norms. Rio de Janeiro. Brazil (In Portuguese).
33. NBR 12653. (2015) NBR 12653 - Pozzolanic materials – Requirements. Brazilian Association of Technical Norms. Rio de Janeiro. Brazil (In Portuguese).
34. Dunnett, C.W. (1955) A multiple comparison procedure for comparing several treatments with a control. *J. Am. Statist. Assoc*. 50, 1096-1121. https://doi.org/10.2307/2281208.
35. Tukey, J.W. (1949) Comparing individual means in the analysis of variance. *Biometrics.* 5, 99-114. https://doi.org/10.2307/3001913.
36. Malaiskiene, J.; Kizinievic, O.; Kizinievic, V.; Boris, R. (2018) The impact of primary sludge from paper industry on the properties of hardened cement paste and mortar. *Construct. Build. Mater.* 172, 553-561. https://doi.org/10.1016/j.conbuildmat.2018.04.011.
37. Martins, R.O.G.; Sant'Ana Alvarenga, R.C.S.; Pedroti, L.G.; de Oliveira, A.F.; Mendes, B.C.; Azevedo, A.R.G. (2018) Assessment of the durability of grout submitted to accelerated carbonation test. *Construct. Build. Mater.* 129 [20], 261-268. https://doi.org/10.1016/j.conbuildmat.2017.10.111.
38. Marliere, E.; Mabrouk, M.; Lamblet, P., Coussot, P. (2012) How water retention in porous media with cellulose ethers works. *Cem. Concr. Res*. 42 [11], 1512-1529. https://doi.org/10.1016/j.cemconres.2012.08.010.
39. Mattana, A.J.; Medeiros, M.H.F.; Silva, N.G.; Costa, M.R.M.M. (2012) Análise hierárquica para escolha entre agregado natural e areia de britagem de rocha para confecção de argamassas de revestimento. *Ambien. Constr.* 12 [4], 63-79. https://doi.org/10.1590/S1678-86212012000400006.
40. Costa, J. S. (2006) Alternative aggregates for mortar and concrete produced from the recycling of virgin waste from the traditional ceramics industry. Thesis (Doctorate), Universidade Federal de São Carlos - UFSCAR, São Carlos, 208p (In Portuguese).
41. Marousek, J.; Haskova S.; Zeman R.; Zak, J.; Vanícková, R.; Marouskova, A.; Vachal, J.; Myskova, J. (2015) Techno-economic assessment of processing the cellulose casings waste. *Clean Technol. Environ. Policy*. 17, 2441-2446. https://doi.org/10.1007/s10098-015-0941-x.
42. Lafhaj, Z.; Goueygou, M.; Djerbi, A.; Kaczmarek M. (2006) Correlation between porosity, permeability and ultrasonic parameters of mortar with variable water/cement ratio and water content. *Cem. Concr. Res.* 36 [4], 625-633. https://doi.org/10.1016/j.cemconres.2005.11.009.
43. Callister, W.D.; Rethwisch, D.G. (2012) Materials science and engineering: An introduction. LTC, v. 8° Edição.
44. Marvila, M.; Alexandre, J.; Rangel, A.A.G.; Zanelato, E.; Monteiro, S.N.; Delaqua, G.; Amaral, L. (2017) Estudo da Capilaridade para Argamassas de Múltiplo uso. *Anais do Congresso Anual da ABM*. 72, 1.
45. Azevedo, A.R.G.; Alexandre, J.; Xavier, G.C.; Pedroti, L.G. (2018) Recycling paper industry effluent sludge for use in mortars: A sustainability perspective. *J. Clean. Produc.* 192, 335-346. https://doi.org/10.1016/j.jclepro.2018.05.011.
46. Azevedo, A.R.G.; Alexandre, J.; Marvila, M.T.; Xavier, G.C.; Monteiro, S.N.; Pedroti, L.G. (2020) Technological and environmental comparative of the processing of primary sludge waste from paper industry for mortar. *J. Clean. Produc.* 249, 119336. https://doi.org/10.1016/j.jclepro.2019.119336.
47. Alves, A. (2018) Determination of physical, chemical and mechanical properties of mortars based on metakaolin activated by NaOH, KOH and NaOH + KOH. Dissertation (Masters in Civil Engineering) – Campos dos Goytacazes, RJ - Universidade Estadual do Norte Fluminense – UENF (In portuguese).
48. Ramalho, M.A.; Corrêa, M.R.S. (2003) Projeto de edifícios de alvenaria estrutural, 1.ed. São Paulo.
49. Ramachandran, V.S.; Paroli, R.M.; Beaudoin, J.J.; Delgado, A.H. (2002) Handbook of thermal analysis of construction materials. William Andrew Publishing/Noyes, Norwich, 491-530.
50. Silva, A.S. (2018) Dolomitic lime: the past and present. *Ambient. Constr.*18 [4], 63-73. https://doi.org/10.1590/s1678-86212018000400293.
51. Santiago, E.I.; Andrade, A.V.C.; Paiva-Santos C.O.; Bulhões L.O.S. (2003) Structural and electrochemical properties of $LiCoO_2$ prepared by combustion synthesis. *Solid State Ionics*. 158, 91-102. https://doi.org/10.1016/S0167-2738(02)00765-8.
52. Malaiškienė, J.; Banevičienė, V.; Boris, R.; Antonovič, V. (2019) The effect of dried paper-mill sludge on cement hydration. *J. Thermal Anal. Calorim.* 138, 4107-4118. https://doi.org/10.1007/s10973-019-08587-w.
53. Mehta, P.K.; Monteiro, P.J.M. (2014) Concreto: microestrutura, propriedades e materiais. 2 ed. São Paulo: IBRACON.